

ADDITIONS AND CORRECTIONS

2003, Volume 107A

W. B. Zeimen, J. Klos, G. C. Groenenboom, and A. van der Avoird*: Bound States of the $\text{Cl}(^2P)\text{-HCl}$ van der Waals Complex from Coupled *ab Initio* Potential Energy Surfaces

Page 5110: Recently we discovered an error in the code of the $\text{Cl}(^2P)\text{-HCl}$ potentials used to generate the bound levels of this complex. The code used to produce the plots of the potentials did not contain this error, and Figures 1 and 2 in the Article are correct. New bound level calculations with the same methods and basis sets as used in the Article are performed on the corrected potentials and reported here.

One-Dimensional Calculations

The results of one-dimensional calculations with the R coordinate fixed with a range of values from 2.5 to 5.5 Å that were shown in Figures 3–5 and in Tables 1 and 2 are presented in Figure 1 of this Erratum. The component analysis of the wave functions at $R = 3.2$ and 3.9 Å in Tables 1 and 2 did not change very much; so we do not include new tables. Also the plots of the 1D wave functions at these values of R in Figures 4 and 5 of the Article did not change much; hence we also refrain from presenting new figures of the 1D wave functions. The energy levels plotted as functions of R in Figure 1 of this Erratum differ strongly from the levels in Figure 3 or the Article, however. We still observe two sets of states: states with a T-shaped geometry that correspond mostly to the diabatic electronic state with $j_A = 3/2$ and $|\omega_A| = 1/2$ and have minima in their effective radial potentials for $R \approx 3.2$ Å and states with a linear geometry that correspond to the diabatic state with $j_A = 3/2$ and $|\omega_A| = 3/2$ and have minima in their radial potentials for $R \approx 3.9$ Å.

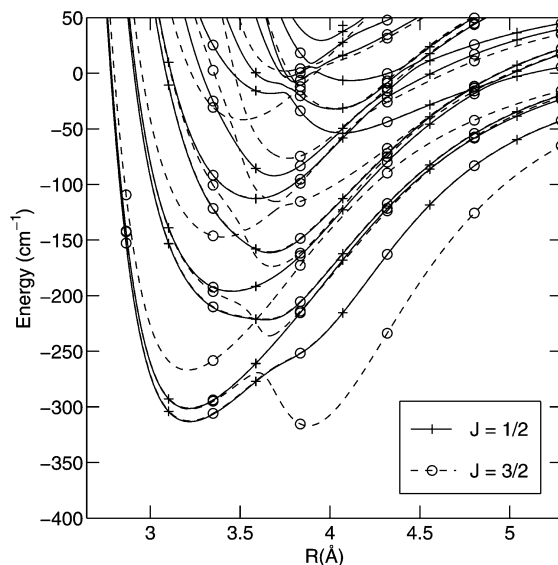


Figure 1. Bound state energies calculated with R fixed at different values. Solid lines with crosses correspond to $J = 1/2$ and dashed lines with circles to $J = 3/2$.

The T-shaped and linear states have very similar binding energies now, in contrast with the incorrect results in the Article for which the T-shaped states had considerably lower energy than the linear states.

Full Calculations

The results from full calculations listed in Tables 3–6 of the Article and the wave functions displayed in Figure 6 of that paper, after correction, are given in Tables 1–4 and in Figures

TABLE 1: Lowest Bound States of e Parity for $J = 1/2$ up to $7/2^a$

$ \omega_A $	$ \omega_B $	v_b	v_s	$J = 1/2$	$J = 3/2$	$J = 5/2$	$J = 7/2$	$ \omega_A $	$ \omega_B $	v_b	v_s	$J = 1/2$	$J = 3/2$	$J = 5/2$	$J = 7/2$
$ \Omega = 1/2$															
$1/2$	0	0	0	-291.0919	-290.9726	-290.6779	-290.2099	$1/2$	0	0	1	-196.1121	-195.9885	-195.7154	-195.2927
$1/2$	1	0	0	-278.7131	-278.3821	-277.8477	-277.1194	$1/2$	1	1	0	-177.7902	-177.3833	-176.8895	-176.2478
$1/2$	0	0	1	-253.1944	-253.0793	-252.8020	-252.3624	$1/2$	0	1	1	-172.0715	-171.9728	-171.7275	-171.3356
$1/2$	1	0	1	-237.8671	-237.6077	-237.1848	-236.5995	$1/2$	0	0	3	-165.4168	-165.2146	-164.8678	-164.3779
$1/2$	0	0	0	-226.4408	-226.3116	-226.0341	-225.6083	$1/2$	1	0	3	-163.4269	-163.2576	-162.9273	-162.4350
$1/2$	0	0	2	-202.0288	-201.9010	-201.6223	-201.1917	$1/2$	1	1	1	-145.4491	-145.1883	-144.7809	-144.2280
$1/2$	1	0	2	-199.8789	-199.6379	-199.2253	-198.6449								
$ \Omega = 3/2$															
$3/2$	0	0	0		-290.7702	-290.4548	-290.0115	$1/2$	2	?	?		-200.5514	-200.1791	-199.6513
$1/2$	1	0	0		-279.4772	-279.1227	-278.6096	$1/2$	1	0	2		-194.3374	-193.9847	-193.4904
$(3/2)/(1/2)$	0/1	0	1		-246.0789	-245.7283	-245.2378	$1/2$	1	1	0		-177.7143	-177.4408	-177.0183
$1/2$	2	0	0		-243.4833	-242.9941	-242.3123	$1/2$	1	?	?		-165.9482	-165.6021	-165.1168
$(3/2)/(1/2)$	0/1	0	1		-233.5762	-233.1972	-232.6650	$1/2$	2	0	2		-161.0318	-160.7026	-160.2301
$1/2$	1/2	?	?		-202.1563	-201.7800	-201.2578	$3/2$	0	1	1		-150.7340	-150.4103	-149.9572
$ \Omega = 5/2$															
$1/2$	2	0	0			-245.1405	-244.5859	$1/2$	2	?	?		-159.8990	-159.2860	
$1/2$	2	0	1			-208.7114	-208.1750	$1/2$	2	1	1		-148.1920	-147.8380	
$(3/2)/(1/2)$	1/2	0	0			-189.4022	-188.8983	$1/2$	3	1	1		-142.3658	-141.7591	
$1/2$	3	0	0			-186.0306	-185.3523								
$ \Omega = 7/2$															
$1/2$	3	0	0				-187.8930	$1/2$	3	1	1				-147.4919

^a Energies in cm^{-1} relative to the energy of $\text{Cl}(^2P_{3/2})$ and HCl ; v_b and v_s are bend and stretch quantum numbers. Question marks indicate that we could not assign v_b and v_s because of strong mixing.

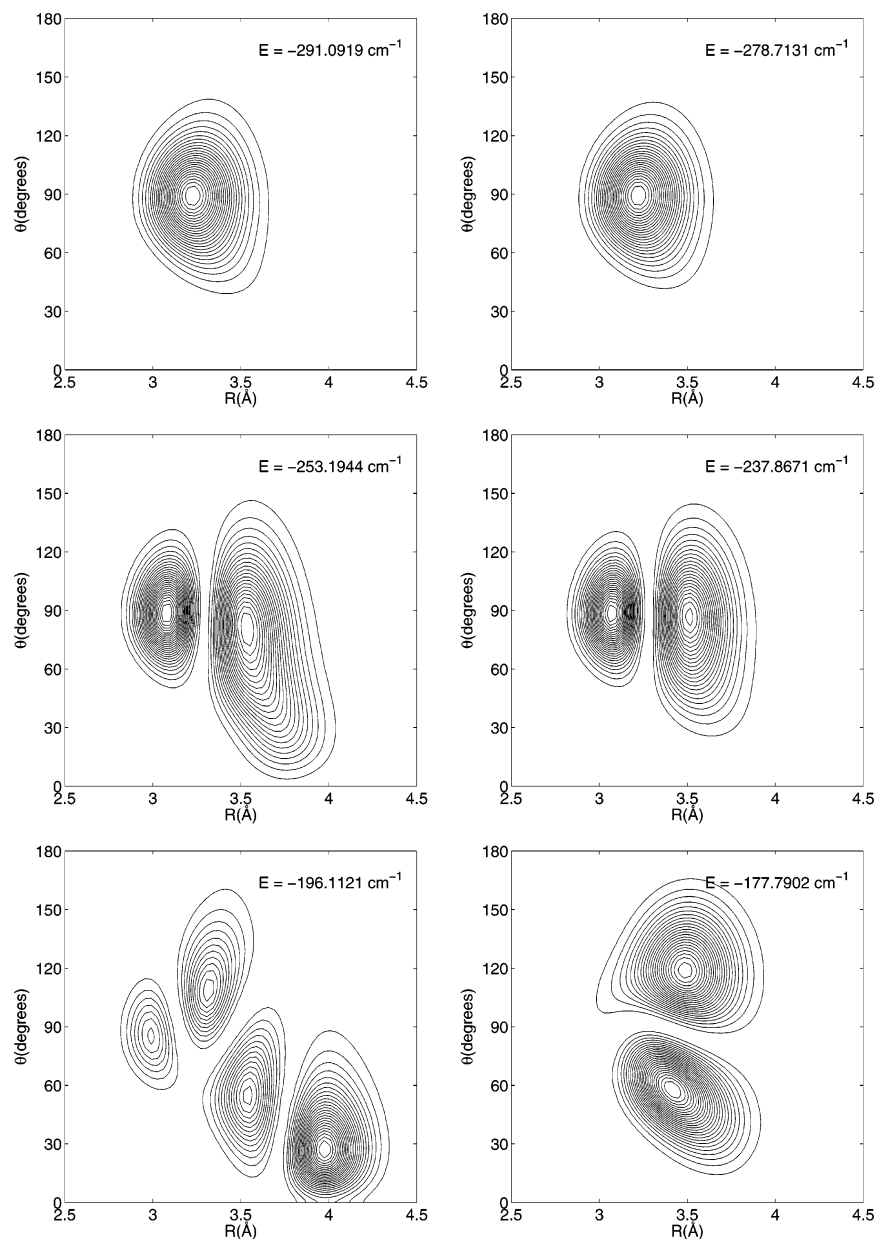


Figure 2. Density distributions from full 2D calculations for $J = 1/2$ and $|\Omega| = 1/2$. These distributions are the squares of the rovibronic wave functions, integrated over the electronic coordinates and the overall rotation angles of the complex (α, β, ϕ) . The corresponding energy levels are listed in Table 1 here.

TABLE 2: Parity Splittings $\Delta E = E_f - E_e$ in cm^{-1}

$ \omega_A $	$ \omega_B $	ν_b	ν_s	$J = 1/2$	$J = 3/2$	$J = 5/2$	$J = 7/2$	$ \omega_A $	$ \omega_B $	ν_b	ν_s	$J = 1/2$	$J = 3/2$	$J = 5/2$	$J = 7/2$
$ \Omega = 1/2$															
$1/2$	0	0	0	0.2865	0.5764	0.8666	1.1598	$1/2$	0	0	1	0.2011	0.4020	0.6024	0.8022
$1/2$	1	0	0	-0.0140	-0.0273	-0.0402	-0.0530	$1/2$	1	1	0	-0.0500	-0.0533	-0.0920	-0.1353
$1/2$	0	0	1	0.2564	0.5125	0.7682	1.0232	$1/2$	0	1	1	0.2418	0.4835	0.7247	0.9653
$1/2$	1	0	1	-0.0265	-0.0528	-0.0785	-0.1034	$1/2$	0	0	3	0.0370	0.0771	0.1232	0.1772
$1/2$	0	0	0	0.1866	0.3732	0.5596	0.7458	$1/2$	1	0	3	0.1389	0.2746	0.4044	0.5257
$1/2$	0	0	2	0.1959	0.3909	0.5838	0.7731	$1/2$	1	1	1	-0.0788	-0.1565	-0.2320	-0.3041
$1/2$	1	0	2	0.0389	0.0751	0.1069	0.1338								
$ \Omega = 3/2$															
$3/2$	0	0	0	-0.0034	-0.0073	-0.0142		$1/2$	2	?	?		0.0036	0.0134	0.0306
$1/2$	1	0	0	-0.0006	-0.0018	-0.0030		$1/2$	1	0	2		0.0001	0.0005	0.0013
$(3/2)/(1/2)$	0/1	0	1	0.0001	0.0003	0.0008		$1/2$	1	1	0		-0.0468	-0.0583	-0.0651
$1/2$	2	0	0	0.0000	0.0000	0.0000		$1/2$	1	?	?		-0.0001	-0.0004	-0.0005
$(3/2)/(1/2)$	0/1	0	1	-0.0003	-0.0013	-0.0033		$1/2$	2	0	2		0.0002	0.0008	0.0020
$1/2$	1/2	?	?	0.0001	0.0006	0.0022		$3/2$	0	1	1		0.0001	0.0004	0.0010

2 and 3 of this Erratum. We find that the quantum number Ω , the projection of the total angular momentum J of the complex on the dimer bond axis R , remains a nearly good quantum

number. The ground state of the complex has $J = |\Omega| = 1/2$ and is still T-shaped (Figure 2 here). Its electronic wave function has mostly $j_A = 3/2$ and $|\omega_A| = 1/2$ character, as before. The

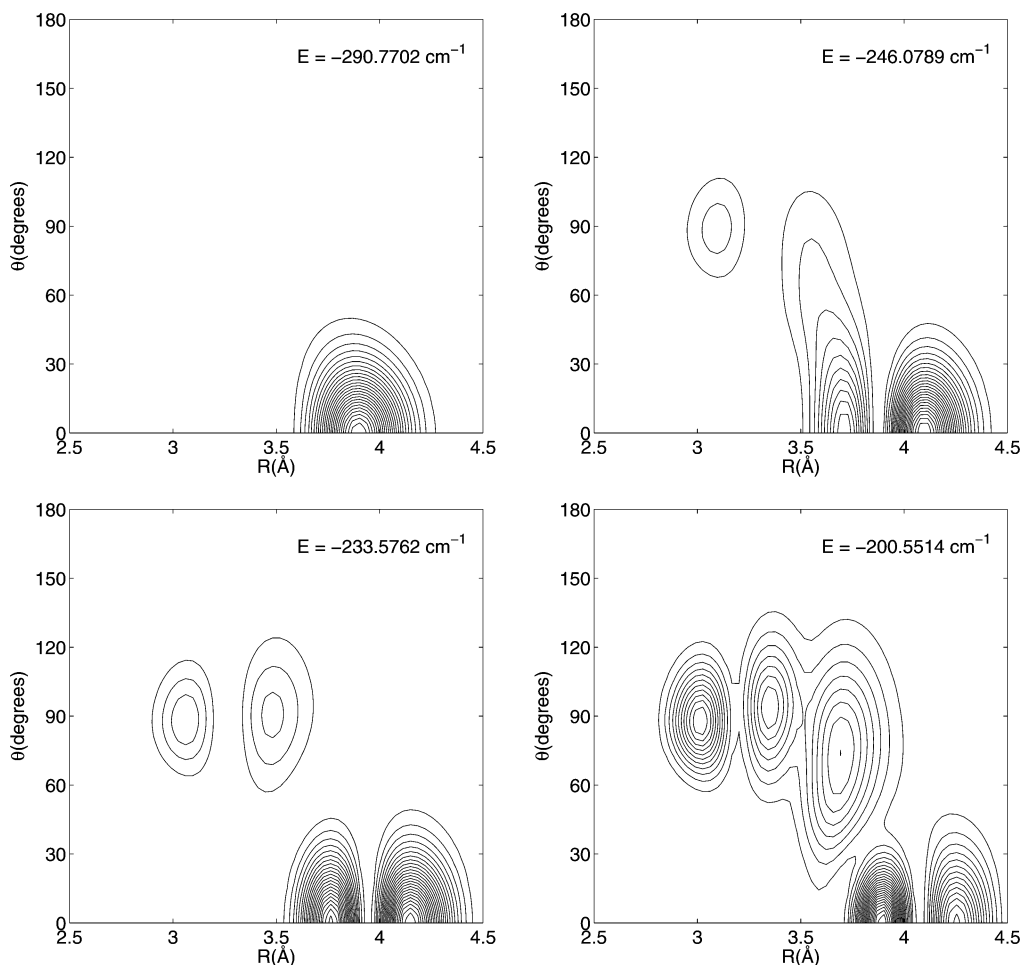


Figure 3. Density distributions from full 2D calculations for $J = 3/2$ and $|\Omega| = 3/2$. The corresponding energy levels are listed in Table 1.

TABLE 3: Spectroscopic Parameters in cm^{-1} from a Fit of the Stretch Progression for $|\Omega| = 1/2$ and $|\omega_B| = 1$

D_e	ω_e	$\omega_e x_e$	$\omega_e y_e$
-300.6033	44.9044	2.3844	0.2167

dissociation energy D_0 is 291.1 cm^{-1} , and the van der Waals bond length R is approximately 3.2 \AA . The lowest state with $J = |\Omega| = 3/2$, the wave function of which is displayed in the first panel of Figure 3 here, has a linear geometry and mostly $j_A = |\omega_A| = 3/2$ character. The corresponding van der Waals bond length R equals approximately 3.9 \AA , and the binding energy D_0 of this linear state is 290.8 cm^{-1} , very nearly the same as for the T-shaped ground state. We remind the reader that the deepest well in the lowest adiabatic potential including spin-orbit coupling is 439 cm^{-1} for the linear geometry, whereas the depth of the well for the T-shaped geometry is only 377 cm^{-1} ; see Figure 1 of the Article. Obviously, the smaller well depth for the T-shaped geometry is just compensated by a lower zero-point energy of the T-shaped complex.

A number of stretch and bending excited states with $J = |\Omega| = 1/2$ also have the T-shaped geometry (Figure 2 here). Other excited states are mixed; they are delocalized over T-shaped and linear geometries (see, for example, the state at $-196.1121 \text{ cm}^{-1}$ in Figure 2). Some of the states with $|\Omega| = 1/2$ have the same approximate quantum numbers; see Table 1 of this Erratum. They always occur pairwise: the lower state is T-shaped, and the higher one has predominantly the linear geometry. The excited states with $|\Omega| = 3/2$ have an even stronger tendency to mix than the states with $|\Omega| = 1/2$ (Figure 3 here). This mixing has become much more pronounced after

correction of the potential because the energy gap between the T-shaped and linear states is much smaller than it was with the uncorrected potential. In a number of cases indicated with a question mark in Table 1 here we could not assign stretch or bend quantum numbers, because of substantial delocalization over the T-shaped and linear geometries. Because the mixing in the wave functions from the full calculations involves T-shaped structures centered around $R = 3.2 \text{ \AA}$ and linear structures centered around $R = 3.9 \text{ \AA}$, it did not occur as strongly in the 1D calculations with R fixed at either one of these values.

A typical feature that remains is that the Cl-HCl complex has two series of states with a T-shaped geometry and $|\Omega| = 1/2$ with similar internal motion, one series with $\omega_B \approx 0$ that includes the ground state at -291.1 cm^{-1} , and one series with $|\omega_B| \approx 1$ that starts at the slightly higher energy of -278.7 cm^{-1} . Stretch excited levels of T-shaped geometry can be identified, but the stretch progressions have become very irregular after correction of the potential except for the levels with $|\Omega| = 1/2$ and $|\omega_B| \approx 1$. The fit of these levels to eq 11 of the Article yields the spectroscopic parameters given in Table 3 here. A bend excited state of T-shaped geometry can be identified as well but does not show a regular stretch progression. Stretch excited states of linear geometry are found too, but do not show a regular progression because of strong mixing with T-shaped states.

The large parity splittings found for $|\Omega| = 1/2$ are still nicely proportional to $J + 1/2$. Their values in Table 2 changed only little for the lower states; for some of the higher states the changes are larger. Another remarkable feature remains: the $\omega_B = 0$ states of Cl-HCl for which we find this large parity

TABLE 4: Expectation Values and Spectroscopic Parameters in cm^{-1} from Fits of the Rotational Levels

$ \omega_A $	$ \omega_B $	ν_b	ν_s	$\langle R \rangle$ (\AA)	B_{av}	E_0	B	D
					$ \Omega = 1/2$			
$1/2$	0	0	0	3.29	0.08857	-290.9928	0.08815	1.49×10^{-5}
$1/2$	1	0	0	3.28	0.08900	-278.7740	0.10865	2.33×10^{-4}
$1/2$	0	0	1	3.45	0.08151	-253.1068	0.08107	3.00×10^{-6}
$1/2$	1	0	1	3.40	0.08388	-237.9214	0.08215	1.30×10^{-5}
$1/2$	0	0	0	3.63	0.07401	-226.3845	0.07415	6.35×10^{-7}
$1/2$	0	0	2	3.54	0.07748	-201.9683	0.07507	1.70×10^{-6}
$1/2$	1	0	2	3.51	0.07918	-199.9027	0.08664	7.60×10^{-5}
$1/2$	0	0	1	3.64	0.07414	-196.0488	0.07467	2.71×10^{-7}
$1/2$	1	1	0	3.50	0.07835	-177.8618	0.12589	1.70×10^{-3}
$1/2$	0	1	1	3.67	0.07245	-171.9872	0.07320	1.85×10^{-6}
$1/2$	0	0	3	3.65	0.07465	-165.4353	0.07412	1.18×10^{-5}
$1/2$	1	0	3	3.64	0.07507	-163.3969	0.07906	2.62×10^{-6}
$1/2$	1	1	1	3.61	0.07484	-145.5255	0.07403	8.31×10^{-6}
					$ \Omega = 3/2$			
$3/2$	0	0	0	3.89	0.06315	-290.8658	0.06258	-1.30×10^{-5}
$1/2$	1	0	0	3.30	0.08815	-279.5818	0.06917	-2.03×10^{-4}
$(3/2)/(1/2)$	0/1	0	1	3.71	0.07137	-246.1841	0.07016	2.09×10^{-6}
$1/2$	2	0	0	3.28	0.08889	-243.6304	0.09813	3.68×10^{-5}
$(3/2)/(1/2)$	0/1	0	1	3.65	0.07420	-233.6897	0.07558	-1.55×10^{-5}
$1/2$	1/2	?	?	3.59	0.07683	-202.2697	0.07569	4.84×10^{-5}
$1/2$	2	?	?	3.49	0.08069	-200.6618	0.07465	-9.86×10^{-5}
$1/2$	1	0	2	3.75	0.06942	-194.4431	0.07049	-9.48×10^{-6}
$1/2$	1	1	0	3.62	0.07431	-177.8129	0.04935	-5.26×10^{-4}
$1/2$	1	?	?	3.65	0.07451	-166.0519	0.06910	-1.13×10^{-5}
$1/2$	2	0	2	3.49	0.08021	-161.1291	0.06476	-1.42×10^{-4}
$3/2$	0	1	1	3.90	0.06586	-150.8311	0.06478	7.93×10^{-7}

splitting that is normally observed in linear open-shell molecules are not linear but have a T-shaped geometry. The much smaller parity splittings that occur for levels with $|\omega_B| > 0$ change drastically.

Table 4 here lists the rotational constants of the complex extracted from the levels with $J = 1/2, 3/2, 5/2, 7/2$ with the use of eq 13 in the Article. This table contains also rotational constants B_{av} computed as expectation values over the wave functions. As before, the agreement between the two values of B is mostly good for the levels with $\omega_B = 0$, somewhat less good for the levels with $|\omega_B| > 0$. On the basis of the rotational constants and the values of $\langle R \rangle$ in Table 4, one can clearly distinguish the T-shaped structures with $\langle R \rangle$ values between 3.2 and 3.5 \AA and the linear structures with $\langle R \rangle$ ranging from 3.7

to 4.0 \AA . Some of the levels are strongly perturbed (see, for example, the levels with $|\Omega| = 1/2$ and $3/2$) at -177.8 cm^{-1} , and the rotational constant B from the fit of the levels differs strongly from the expectation value B_{av} . This perturbation is due to a mixing of T-shaped and linear states that are very near in energy.

Acknowledgment. We thank Ms. Anna Fishchuk for her help in recalculating and analyzing the bound states on the corrected potential surfaces.

10.1021/jp046260a

Published on Web 09/21/2004